HIGH FRACTIONALLY SPACED CONSTANT MODULUS BLIND EQUALIZATION FOR HIGH ORDER-QAM SIGNALLING

A. Zaouche, I. Dayoub, and J. M. Rouvaen

Institut d'Electronique de Microelectronique et de Nanotechnologie IEMN
DOAE UMR CNRS 8520 universit$\acute{e}$ de valenciennes-Le Mont Houy
59313 valenciennes Cedex 9 -France-

ABSTRACT

Blind channel equalization has gained a wide-spread use in communications systems. This type of equalization doesn't make use of any training sequence. The most commonly used blind adaptation algorithm is known as the *constant modulus algorithm* (CMA). The present paper presents the performances of fractionally spaced constant modulus equalization applied for 256-QAM and 1024-QAM modulated signals. Two ways of sampling the received data are investigated. The very known $\frac{T}{2}$FSE where the received signals are sampled at rate twice the baud rate and $\frac{T}{8}$FSE where the received signal is sampled at rates which are eight times the baud rate.

1. INTRODUCTION

Due to the increase in data transmission rates more efficient spectral methods of modulating the transmitted signals such as 256-QAM and 1024-QAM are required. However, increasing the modulation scheme levels causes a severe distortions in the received signals after undergoing all the degradation phenomena due to the band limiting effect of the channel and the multi-path propagation [6]. Thus, the signal recovery would be a tedious task to achieve. To overcome this problem equalizers are proposed. Blind equalizers are preferred over trained equalizers because they are not bandwidth consuming [7]. They make use only of statistical properties of the input signal and the noise. The most commonly used blind adaptive algorithm is referred as *constant modulus algorithm* (CMA) [5],[6],[7] .This algorithm makes use of the *constant modulus* (CM) criterion which penalizes the deviation of the magnitude of the received data from a desired amplitude level [1],[5]. CMA can be used also for a non constant modulus sources such as QAM modulated signals which is the modulation type used in this paper. Most often, channels are represented by *finite impulse response* (FIR) filters. This causes FIR equalization in the baud case where, the tap spacing of the equalizer is the same as the symbol period T to be practically impossible. To overcome this limitation, *fractionally spaced equalization* (FSE) is proposed. FSE uses FIR equalizers whose tap spacing is an integer fraction of the symbol period T. T/2-FSE is the most popular and most studied in literature [1],[3],[5]. But, what will be the effect of increasing the sampling rate in the fractionally spaced equalization on highly M-QAM modulated signals which are relatively difficult to equalize?.*Thus, the objective of the present work is to highlight the effect of increasing the sampling rate of the received signals in FSE when applied to high order QAM signals such as 256-QAM and 1024-QAM*.

2. SYSTEM MODEL

In this paper, we consider a fractionally spaced equalization based on receivers operating at M times the baud rate. The system model under consideration is shown in Fig.1.

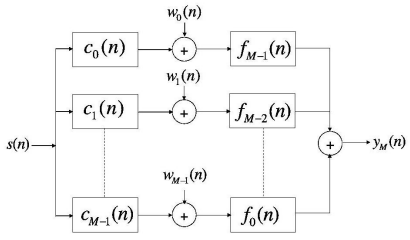

Fig. 1. multi-channel model for T/M-FSE

The multi-channel model of $\frac{T}{M}$ fractionally spaced equalization shows that the equalized received data is obtained after M summations of direct convolutions between baud spaced input data $s(n)$ and M baud spaced sub-channels and M baud spaced sub-equalizers. Let us assume that the corresponding FIR channel and FSE lengths are ML and MN respectively, where L and N are given positive integers. The overall multi-channel convolution matrix **h** can be expressed as:

$$\mathbf{h} = \mathbf{Cf} \tag{1}$$

where, **C** is the fractionally spaced convolution matrix constructed from the baud spaced sub-channels as follows:

$$\mathbf{C} = \begin{bmatrix}\mathbf{C}_0 & \mathbf{C}_1 & \mathbf{C}_2 & \dots & \mathbf{C}_{M-1}\end{bmatrix}_{(P\times MN)} \quad (2)$$

and **f** the fractionally spaced equalizer vector constructed as

$$\mathbf{f} = \begin{bmatrix}\mathbf{f}_0 & \mathbf{f}_1 & \mathbf{f}_2 & \dots & \mathbf{f}_{M-1}\end{bmatrix}_{MN\times 1} \quad (3)$$

Perfect fractionally blind equalization requires from the overall system response to behave as a delay operator and this is achieved under the following conditions

- No channel noise
- Zero mean and independent finite alphabet with sub-gaussian kurtosis (*source kurtosis less than 3 for real sources and less than 2 for complex ones*)
- No common roots between the polynomials formed by the baud spaced sub-channels
- The satisfaction of the *strong perfect equalization condition* which requires from the sylvester matrix **C** to be full-row rank. This condition is satisfied for **C** having the number of columns greater than or equal to the number of rows. This can be formulated in mathematical form as:

$$P = N + L - 1 \leq MN \Rightarrow N \geq \frac{L-1}{M-1} \quad (4)$$

3. FRACTIONALLY SPACED CONSTANT MODULUS ALGORITHM

The CM criterion tries to restore the constant modulus property of the communication signal by penalizing the deviation in the modulus of the received signal [1]. The adaptive CM equalization minimizes a CM cost function given in its more general form as follows

$$J_{CM}^{p,q} = \frac{1}{pq}E\left\{\left||y_n|^p - \gamma\right|^q\right\} \quad (5)$$

where p and q are two positive integers and $\gamma = \frac{E\{|s_n|^4\}}{E\{|s_n|^2\}}$ is the dispersion constant [3]. The CMA equalizer update equation is given as follows:

$$\begin{aligned}\mathbf{f}(n+1) &= \mathbf{f}(n) + \mu\mathbf{r}^*(n)\{-\nabla_{y_n}J_{CM}\} \\ &= \mathbf{f}(n) + \mu\mathbf{r}^*(n)\underbrace{y_n(\gamma - |y_n|^2)}_{\psi(n)}\end{aligned} \quad (6)$$

where $\psi(n)$ is the CM error function and **f** represents the equalizer coefficient vector , μ a small step size and **r** the fractionally spaced regressor vector. The step size requirement in CMA is shown below

$$0 < \mu \leq \frac{2}{(\kappa_g - \kappa_s)\lambda_{max}} \quad (7)$$

where κ_g and κ_s are the normalized kurtosises for the gaussian source and the actual source respectively and λ_{max} is the maximum eigenvalue of the hermitian matrix $\mathbf{C}^H\mathbf{C}$.

4. COST FUNCTION

In this section the shape of the CM cost function given in equation (5) is investigated. Different CM cost functions are obtained for different values of p and q, but in the present work we restrict our analysis to the Godard's 2-2 CM cost function where p and q are both equal to 2. It is given bellow

$$J_{CM}^{2,2} = \frac{1}{4}E\left\{\left||y_n|^2 - \gamma\right|^2\right\} \quad (8)$$

Let's define the variance and the normalized kurtosis of the source sequence $\{s_n\}$ respectively as follows

$$\sigma_s^2 \triangleq E\{|s_n^2|\} \quad (9)$$

$$\kappa_s \triangleq \frac{E\{|s_n|^4\}}{(E\{|s_n|^2\})^2} = \frac{E\{|s_n|^4\}}{\sigma_s^4} \quad (10)$$

and analogously, the variance and the normalized kurtosis for the noise channel sequence $\{w_n\}$ as

$$\sigma_n^2 \triangleq E\{|w_n^2|\} \quad (11)$$

$$\kappa_w \triangleq \frac{E\{|w_n|^4\}}{(E\{|w_n|^2\})^2} = \frac{E\{|w_n|^4\}}{\sigma_w^4} \quad (12)$$

Table I shows the normalized kurtosis for some $M-QAM$ sources [1]. It can be noticed that the source kurtosis for QAM sources gets high as the modulation level increases and approaches its critical value which is 2 corresponding to the normalized kurtosis of a complex gaussian source. This is mainly due to the fact that as the order of QAM signals increases considerably the probability distribution of the constellation points diverges seriously from the uniform distribution and has a tendency to reach the normal distribution. Fractionally spaced blind equalization is practically impossible for complex gaussian source that's why in the present work we focus on compromising between the use of high order QAM modulated input signals which are quite difficult to equalize and the use of high fractionally spaced constant modulus blind equalization which

Table 1. Normalized source kurtosis for $M-QAM$ sources

complex valued $M-QAM$ source	kurtosis
uniform 16-QAM	1.32
uniform 64-QAM	1.381
uniform 256-QAM	1.395
uniform 1024-QAM	1.399

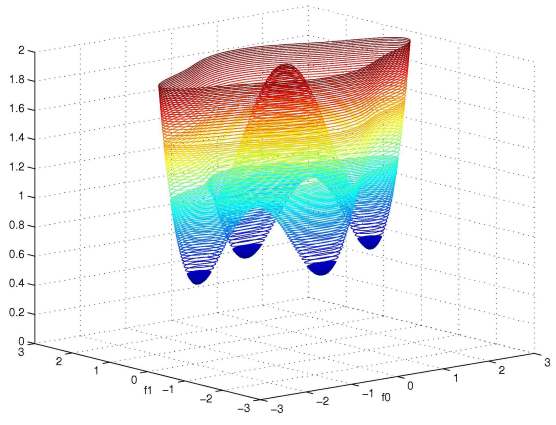

Fig. 2. CMA cost function in no noise for well-behaved channel in equalizer space (kurtosis=1.399)

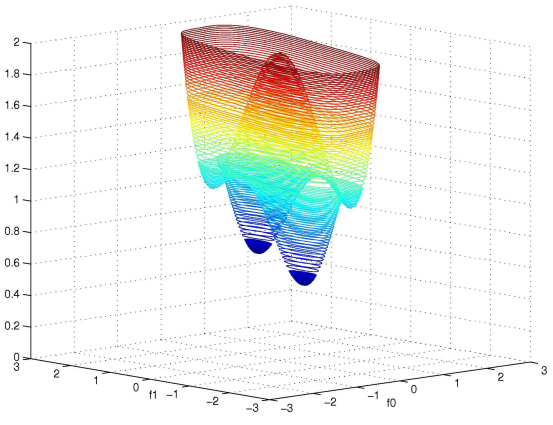

Fig. 3. CMA cost function in no noise for undermodelled channel in equalizer space (kurtosis=1.399)

improves considerably the performances of the blind equalization process.

The CM cost function given in equation (8) has been developed in prior works [4]. For QAM sources and rotationally invariant complex valued *additive white gaussian noise* (AWGN), the cost function is given in [4] as follows

$$\begin{aligned} 4J_{CM} &= (\kappa_s - 2)\sum_{i=0}^{P-1}|h_i|^4 + 2\|\mathbf{h}\|_2^4 + 2\sigma_w^4\|\mathbf{f}\|_2^4 \\ &+ 4\sigma_w^2\|\mathbf{h}\|_2^2\|\mathbf{f}\|_2^2 - 2\kappa_s(\|\mathbf{h}\|_2^2 + \sigma_w^2\|\mathbf{f}\|_2^2) \\ &+ \kappa_s^2 \end{aligned} \quad (13)$$

Fig.2 shows a mesh contour representation of the above CM cost function in noiseless environment for $\frac{T}{2}$FSE in 2 taps equalizer space for kurtosis=1.399 corresponding to the kurtosis of 1024-QAM as shown in table I. The used channel is a well-behaved one given in table II which means that it doesn't have any common sub-channel roots and also the length channel condition for strong perfect equalization is verified (see equation 4). It can be noticed that the CM cost function has a good symmetrical multimodal structure with a four local minima.

In the counterpart Fig.3 shows clearly the effects of violating the channel length condition on the shape of the CM cost function. Refereing to equation(4), it can be easily verified that for a two tap $\frac{T}{2}$ FSE we have $M = 2$ and $N = 1$ and the requirement for L is $L \leq 2$ which requires from the channel length to be less or equal than 4. This condition is violated by using the undermodelled channel shown in table II, where the corresponding length is two taps more than the required one. Fig.3 represents the CM contour mesh representation in noiseless environment in equalizer space for $\frac{T}{2}$FSE with source kurtosis=1.399 and under the undermodelled channel. The CM cost function still has a multimodal symmetrical structure with four local minima having significantly different heights. It can be noticed that for both CM cost figures the MSE is moving away from zero as the source kurtosis increases.

Table 2. Two types of channel impulse responses

channel impulse response	type
[0.0195 0.485 1.03 -0.097]	well-behaved
[0.25 -0.5 0.1 0.95 -0.37 0.6]	undermodelled

5. MEAN SQUARE ERROR CRITERION

Under the assumptions that the noise and source are i.i.d and jointly incorrelated the source normalized minimum square error function is given below [1]

$$J_{MSE} = (\mathbf{Cf} - \mathbf{h}_\delta)^H(\mathbf{Cf} - \mathbf{h}_\delta) + \lambda\mathbf{f}^H\mathbf{f} \quad (14)$$

where $\lambda = \frac{\sigma_w^2}{\sigma_s^2}$ is the ratio between the noise and source variances. The vector that minimizes the above function is $\mathbf{f}^\dagger = \mathbf{A}^{-1}\mathbf{C}^H\mathbf{h}_\delta$ where, $\mathbf{A} = \mathbf{C}^H\mathbf{C} + \lambda\mathbf{I}$. Replacing the optimal equalizer vector in equation (14) results in the optimal mean squared error given below

$$J_{MSE}(\mathbf{f}^\dagger, \delta) = \mathbf{h}_\delta^H(\mathbf{I} - \mathbf{C}\mathbf{A}^{-1}\mathbf{C}^H)\mathbf{h}_\delta \quad (15)$$

The corresponding optimal system delay can be expressed as

$$\delta^\dagger = argmin\left(\left[\mathbf{I} - \mathbf{C}\mathbf{A}^{-1}\mathbf{C}^H\right]_{\delta,\delta}\right) \quad (16)$$

Fig.4 shows the behavior of the optimal mean square error when varying both the system delay δ and the *signal to noise ratio* (SNR) for $\frac{T}{2}$FSE using SPIB[1] channel 6.

[1]The SPIB data base resides at http://spib.rice.edu/spib/microwave.html

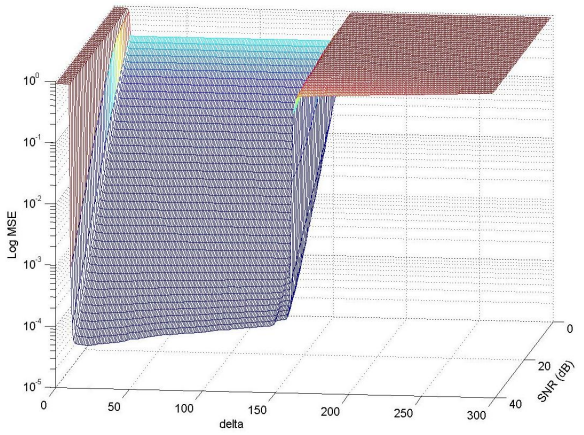

Fig. 4. $J_{MSE}(\mathbf{f}^{\dagger}, \delta)$ versus delay δ and SNR for channel 6

6. SIMULATION

This section deals with the simulation results obtained for $\frac{T}{2}$ FSE and $\frac{T}{8}$ FSE for both 256-QAM and 1024-QAM. Fig.5(a) and Fig.6(a) show the SPIB channel impulse responses for channel 1 and channel 6 respectively that have been used in simulation. The simulation parameters are as follows: the used modulations are 256-QAM and 1024-QAM, SNR=30dB, step size $\mu = 0.0002$, the equalizer length 30, and the iteration number is 100000. The type of channel initialization is a double spike one with only two central taps equal to one and all remaining taps set to zeroes. $\frac{T}{2}$FSE and $\frac{T}{8}$FSE square error histories for both modulation types 256-QAM and 1024-QAM using SPIB channel 1 and channel 6 are shown in Fig.5(b) and Fig.6(b) respectively. It can be noticed that the two modulation schemes do not affect too much the performances of the two fractionally spaced equalizers whereas the choice of the order of sampling the received data is of great interest in improving the performances of the constant modulus fractionally spaced equalization process . The simulation graphs show that for both modulation types and under SPIB channel 1 the mean square error reaches its minimum value at around -26dB for $\frac{T}{2}$FSE and around -32 dB for $\frac{T}{8}$ FSE after 20000 iterations, while under channel 6 the minimum reachable value corresponds to around -25 dB for $\frac{T}{2}$ FSE and -32dB for $\frac{T}{8}$FSE. Fig.5(c) and Fig.5(d) compare the constellation diagrams of 256-QAM for both $\frac{T}{2}$FSE and $\frac{T}{8}$FSE under channel 1 and the above simulation conditions. The improvement brought in the performances of the constant modulus blind fractionally spaced equalization while using $\frac{T}{8}$FSE instead of $\frac{T}{2}$FSE can be easily seen from the constellation diagrams.The same remark can be deduced for channel 6 by exploring the corresponding 256-QAM constellation diagrams shown in Fig.6(c) and Fig.6(d).

7. CONCLUSION

In the present work the performances of high constant modulus blind fractionally spaced equalization that uses high order QAM sources (256-QAM and 1024-QAM) have been investigated. The equalization process performs well as the equalizer sampling rate increases.

8. REFERENCES

[1] C. R. Johnson, Jr. , P. Schniter, T. J. Endres, J. D. Behm, D. R. Brown and R. A. Casas, *"Blind Equalization Using the constant modulus criterion"*, Proc. IEEE oct 1998.

[2] P. Schniter, C. R. Johnson and Jr, *"Dithered signed-error CMA: Robust,Computationally efficient Blind adaptive equalization"*,IEEE transaction on signal processing nov 1998

[3] D. R. Brown, P. B. Schniter and C. R. Johnson, Jr *"Computationally efficient blind equalization"*Allerton conference on communication control and computing 1997

[4] P. B. Schniter *"J_{CM} and $\nabla_f(J_{CM})$:Three important cases"*, February 1998

[5] C. R. Johnson, Jr, P. Schniter, I. Fijalkow, L. Tong, J. D. Brown, R. A. Casas, T. J. Endres, S. Lambotharan, A. Touzni, H. H. Zeng, M. Green and J. R. Treichler *"The core of FSE-CMA behavior theory"* New York , 1999

[6] M. Rupi, P. Tsakalides, E. Del Re and C. L. Nikias *"constant modulus blind equalization based on fractional lower order statistics"*, Signal Processing, 84: 881-894 , 2004

[7] S. Chen, T. B. Cook and L. C. Anderson *"A comparative study of two blind FIR equalizers"*, Digital Signal Processing , 14: 18-36, 2004

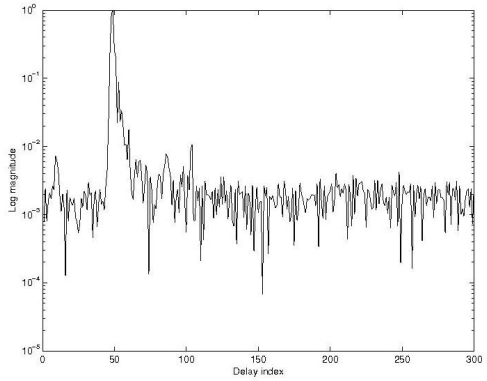

(a) SPIB channel 1

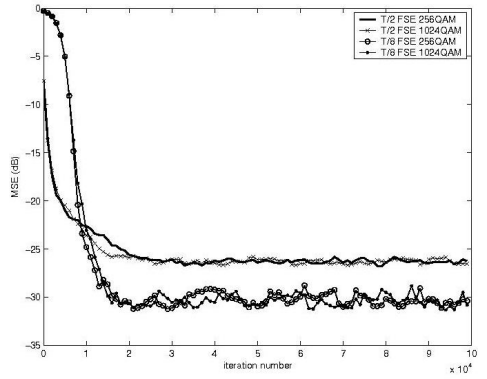

(b) Square error histories for 256-QAM and 1024-QAM using T/2 FSE and T/8 FSE

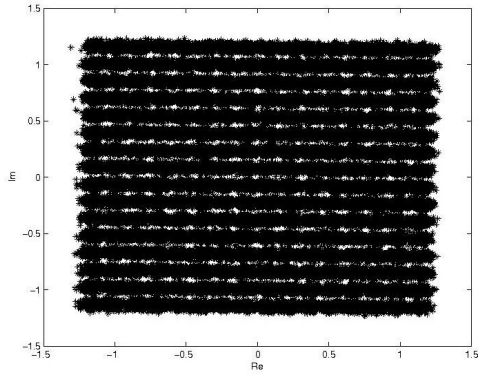

(c) 256-QAM constellation for T/2 FSE

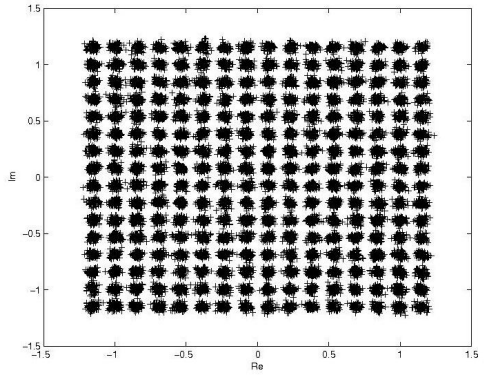

(d) 256-QAM constellation for T/8 FSE

Fig. 5. Simulation results for channel 1

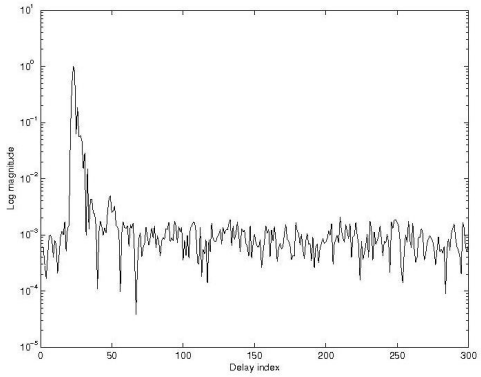

(a) SPIB channel 6

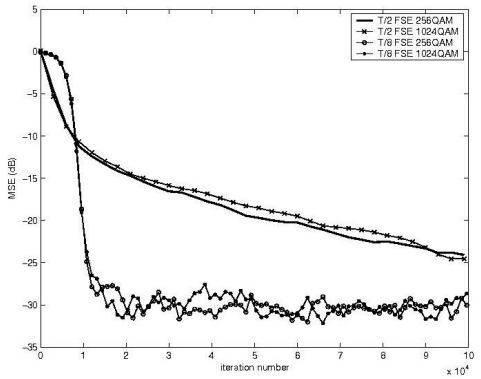

(b) Square error histories for 256-QAM and 1024-QAM using T/2 FSE and T/8 FSE

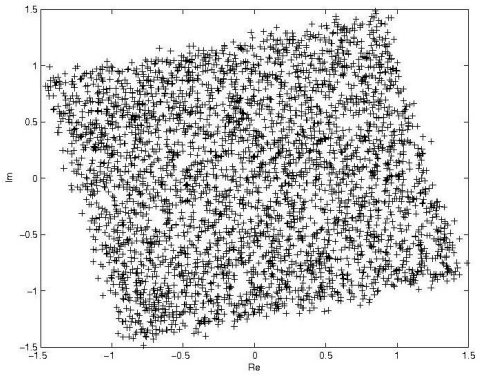

(c) 256-QAM constellation for T/2 FSE

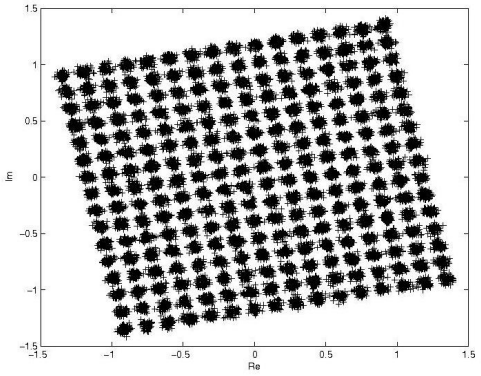

(d) 256-QAM constellation for T/8 FSE

Fig. 6. Simulation results for channel 6